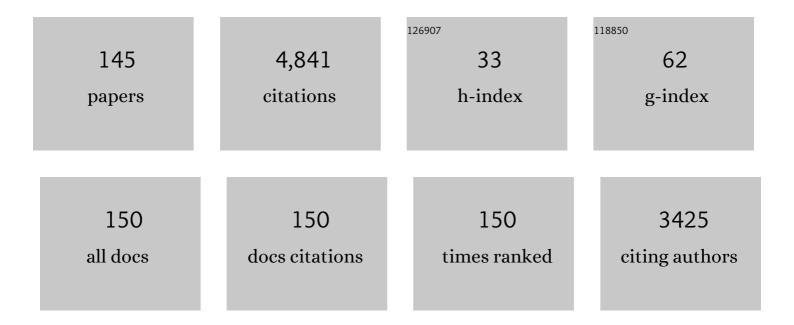
Jens Gutzmer

List of Publications by Year in descending order

Source: https://exaly.com/author-pdf/2890443/publications.pdf Version: 2024-02-01



IENS CUTZMED

#	Article	IF	CITATIONS
1	Timing of magmatic-hydrothermal activity in the Variscan Orogenic Belt: LA-ICP-MS U–Pb geochronology of skarn-related garnet from the Schwarzenberg District, Erzgebirge. Mineralium Deposita, 2022, 57, 1071-1087.	4.1	12
2	Breakup with benefits - hydrothermal mineral systems related to the disintegration of a supercontinent. Earth and Planetary Science Letters, 2022, 580, 117373.	4.4	20
3	Testing the robustness of particle-based separation models for the magnetic separation of a complex skarn ore. International Journal of Mining Science and Technology, 2022, , .	10.3	2
4	A particle-based approach to predict the success and selectivity of leaching processes using ethaline - Comparison of simulated and experimental results. Hydrometallurgy, 2022, 211, 105869.	4.3	3
5	Towards a sampling protocol for the resource assessment of critical raw materials in tailings storage facilities. Journal of Geochemical Exploration, 2022, 236, 106974.	3.2	12
6	A self-adaptive particle-tracking method for minerals processing. Journal of Cleaner Production, 2021, 279, 123711.	9.3	18
7	Geology and Genesis of the Giant Gorevskoe Pb-Zn-Ag Deposit, Krasnoyarsk Territory, Russia. Economic Geology, 2021, 116, 719-746.	3.8	3
8	The Niederschlag fluorite-(barite) deposit, Erzgebirge/Germany—a fluid inclusion and trace element study. Mineralium Deposita, 2021, 56, 1071-1086.	4.1	25
9	Stratigraphy, Depositional Setting, and SHRIMP U-Pb Geochronology of the Banded Iron Formation–Bearing Bailadila Group in the Bacheli Iron Ore Mining District, Bastar Craton, India. Journal of Geology, 2021, 129, 115-130.	1.4	2
10	Mineralogy and fluid characteristics of the Waschleithe Zn skarn – a distal part of the Schwarzenberg mineral system, Erzgebirge, Germany. Ore Geology Reviews, 2021, 131, 104007.	2.7	10
11	Uncertainties in quantitative mineralogical studies using scanning electron microscope-based image analysis. Minerals Engineering, 2021, 167, 106836.	4.3	20
12	Li-Co–Ni-Mn-(REE) veins of the Western Erzgebirge, Germany—a potential source of battery raw materials. Mineralium Deposita, 2021, 56, 1223-1238.	4.1	4
13	Vertical Zoning in Hydrothermal U-Ag-Bi-Co-Ni-As Systems: A Case Study from the Annaberg-Buchholz District, Erzgebirge (Germany). Economic Geology, 2021, 116, 1893-1915.	3.8	10
14	Computing single-particle flotation kinetics using automated mineralogy data and machine learning. Minerals Engineering, 2021, 170, 107054.	4.3	10
15	Spatial and Temporal Evolution of the Freiberg Epithermal Ag-Pb-Zn District, Germany. Economic Geology, 2021, 116, 1649-1667.	3.8	15
16	Timing of native metal-arsenide (Ag-Bi-Co-Ni-As±U) veins in continental rift zones – In situ U-Pb geochronology of carbonates from the Erzgebirge/Krušné Hory province. Chemical Geology, 2021, 584, 120476.	3.3	7
17	Gold and silver deportment in sulfide ores – A case study of the Freiberg epithermal Ag-Pb-Zn district, Germany. Minerals Engineering, 2021, 174, 107235.	4.3	5
18	Genesis of sulfide vein mineralization at the Sakatti Ni-Cu-PGE deposit, Finland. Canadian Mineralogist, 2021, 59, 1485-1510.	1.0	0

#	Article	IF	CITATIONS
19	Not all Neoproterozoic iron formations are glaciogenic: Sturtian-aged non-Rapitan exhalative iron formations from the Arabian–Nubian Shield. Mineralium Deposita, 2020, 55, 577-596.	4.1	17
20	Life on a Mesoarchean marine shelf – insights from the world's oldest known granular iron formation. Scientific Reports, 2020, 10, 10519.	3.3	5
21	Fractionation of geochemical twins (Zr/Hf, Nb/Ta and Y/Ho) and HREE-enrichment during magmatic and metamorphic processes in peralkaline nepheline syenites from Norra Kä (Sweden). Lithos, 2020, 372-373, 105667.	1.4	5
22	Drill-Core Mineral Abundance Estimation Using Hyperspectral and High-Resolution Mineralogical Data. Remote Sensing, 2020, 12, 1218.	4.0	18
23	Supply of Raw Materials and Effects of the Global Economy. , 2019, , 23-105.		2
24	The Raw Material Requirements for Energy Systems. , 2019, , 145-168.		3
25	Constraining the Economic Potential of By-Product Recovery by Using a Geometallurgical Approach: The Example of Rare Earth Element Recovery at Catalão I, Brazil. Economic Geology, 2019, 114, 1555-1568.	3.8	7
26	Automated SEM Mineral Liberation Analysis (MLA) with Generically Labelled EDX Spectra in the Mineral Processing of Rare Earth Element Ores. Minerals (Basel, Switzerland), 2019, 9, 527.	2.0	36
27	Optimal sensor selection for sensor-based sorting based on automated mineralogy data. Journal of Cleaner Production, 2019, 234, 1144-1152.	9.3	17
28	The essence of time – fertile skarn formation in the Variscan Orogenic Belt. Earth and Planetary Science Letters, 2019, 519, 165-170.	4.4	42
29	Stochastic Modeling of Multidimensional Particle Properties Using Parametric Copulas. Microscopy and Microanalysis, 2019, 25, 720-734.	0.4	18
30	Mineral Mapping and Vein Detection in Hyperspectral Drill-Core Scans: Application to Porphyry-Type Mineralization. Minerals (Basel, Switzerland), 2019, 9, 122.	2.0	24
31	The use of assay data as a foundation for a geometallurgical model—The case of the Thaba Chromite Mine, South Africa. Journal of Geochemical Exploration, 2019, 201, 99-112.	3.2	7
32	Indium-bearing sulfides from the Hänmerlein skarn deposit, Erzgebirge, Germany:Âevidence for late-stage diffusion of indium into sphalerite. Mineralium Deposita, 2019, 54, 175-192.	4.1	51
33	Multivariate geochemical classification of chromitite layers in the Bushveld Complex, South Africa. Applied Geochemistry, 2019, 103, 106-117.	3.0	6
34	The Raw Materials Summit 2019: connecting innovation in the Raw Materials Sector. Mineral Economics, 2019, 32, 379-381.	2.8	0
35	Age and genesis of polymetallic veins in the Freiberg district, Erzgebirge, Germany: constraints from radiogenic isotopes. Mineralium Deposita, 2019, 54, 217-236.	4.1	21
36	Trace element geochemistry of sphalerite in contrasting hydrothermal fluid systems of the Freiberg district, Germany: insights from LA-ICP-MS analysis, near-infrared light microthermometry of sphalerite-hosted fluid inclusions, and sulfur isotope geochemistry. Mineralium Deposita, 2019, 54, 237-262.	4.1	122

#	Article	IF	CITATIONS
37	An introduction to the thematic issue on "Ore deposits in the Variscan basement of Central Europe― Mineralium Deposita, 2019, 54, 153-154.	4.1	1
38	The geometallurgical assessment of by-products—geochemical proxies for the complex mineralogical deportment of indium at Neves-Corvo, Portugal. Mineralium Deposita, 2019, 54, 959-982.	4.1	34
39	Genesis of hydrothermal silver-antimony-sulfide veins of the BrÃ ¤ nsdorf sector as part of the classic Freiberg silver mining district, Germany. Mineralium Deposita, 2019, 54, 263-280.	4.1	20
40	The inherent link between ore formation and geometallurgy as documented by complex tin mineralization at the Hämmerlein deposit (Erzgebirge, Germany). Mineralium Deposita, 2019, 54, 683-698.	4.1	10
41	Major and trace element geochemistry of the European Kupferschiefer – an evaluation of analytical techniques. Geochemistry: Exploration, Environment, Analysis, 2018, 18, 132-141.	0.9	6
42	Calculating the deportment of a fine-grained and compositionally complex Sn skarn with a modified approach for automated mineralogy. Minerals Engineering, 2018, 116, 213-225.	4.3	31
43	Quantitative mineralogical analysis of European Kupferschiefer ore. Minerals Engineering, 2018, 115, 21-32.	4.3	25
44	Recovery potential of flotation tailings assessed by spatial modelling of automated mineralogy data. Minerals Engineering, 2018, 116, 143-151.	4.3	17
45	Variation in Platinum Group Mineral and Base Metal Sulfide Assemblages in the Lower Group Chromitites of the Western Bushveld Complex, South Africa. Canadian Mineralogist, 2018, 56, 723-743.	1.0	10
46	Hydrothermal formation of heavy rare earth element (HREE)–xenotime deposits at 100 °C in a sedimentary basin. Geology, 2018, 46, 263-266.	4.4	25
47	Description of Ore Particles from X-Ray Microtomography (XMT) Images, Supported by Scanning Electron Microscope (SEM)-Based Image Analysis. Microscopy and Microanalysis, 2018, 24, 461-470.	0.4	32
48	The South Um Mongul Cu-Mo-Au prospect in the Eastern Desert of Egypt: From a mid-Cryogenian continental arc to Ediacaran post-collisional appinite-high Ba-Sr monzogranite. Ore Geology Reviews, 2017, 80, 250-266.	2.7	29
49	New insights into the petrogenesis of the Jameson Range layered intrusion and associated Fe-Ti-P-V-PGE-Au mineralisation, West Musgrave Province, Western Australia. Mineralium Deposita, 2017, 52, 233-255.	4.1	12
50	Advanced Identification and Quantification of In-Bearing Minerals by Scanning Electron Microscope-Based Image Analysis. Microscopy and Microanalysis, 2017, 23, 527-537.	0.4	36
51	Quantifying the relative availability of high-tech by-product metals – The cases of gallium, germanium and indium. Resources Policy, 2017, 52, 327-335.	9.6	91
52	Distinguishing Magmatic and Metamorphic Processes in Peralkaline Rocks of the Norra Kä Complex (Southern Sweden) Using Textural and Compositional Variations of Clinopyroxene and Eudialyte-group Minerals. Journal of Petrology, 2017, 58, 361-384.	2.8	15
53	Genesis of the Carbonate-Hosted Tres Marias Zn-Pb-(Ge) Deposit, Mexico: Constraints from Rb-Sr Sphalerite Geochronology and Pb Isotopes. Economic Geology, 2017, 112, 1075-1088.	3.8	28
54	Raw material â€~criticality'—sense or nonsense?. Journal Physics D: Applied Physics, 2017, 50, 123002.	2.8	94

#	Article	IF	CITATIONS
55	Oncoidal granular iron formation in the Mesoarchaean Pongola Supergroup, southern Africa: Textural and geochemical evidence for biological activity during iron deposition. Geobiology, 2017, 15, 731-749.	2.4	25
56	Strategic evaluations and mining process optimization towards a strong global REE supply chain. Journal of Sustainable Mining, 2016, 15, 26-35.	0.2	21
57	A mineral liberation study of grain boundary fracture based on measurements of the surface exposure after milling. International Journal of Mineral Processing, 2016, 156, 3-13.	2.6	35
58	MLA-based partition curves for magnetic separation. Minerals Engineering, 2016, 94, 94-103.	4.3	35
59	On the current and future availability of gallium. Resources Policy, 2016, 47, 38-50.	9.6	85
60	Gallium, germanium, indium, and other trace and minor elements in sphalerite as a function of deposit type — A meta-analysis. Ore Geology Reviews, 2016, 76, 52-78.	2.7	269
61	A Review of Graphite Beneficiation Techniques. Mineral Processing and Extractive Metallurgy Review, 2016, 37, 58-68.	5.0	129
62	Rare Earth Underground Mining Approaches with Respect to Radioactivity Control and Monitoring Strategies. , 2016, , 121-138.		4
63	Assessing the supply potential of high-tech metals – A general method. Resources Policy, 2015, 46, 45-58.	9.6	30
64	Efficient and Accurate Identification of Platinum-Group Minerals by a Combination of Mineral Liberation and Electron Probe Microanalysis with a New Approach to the Offline Overlap Correction of Platinum-Group Element Concentrations. Microscopy and Microanalysis, 2015, 21, 1080-1095.	0.4	25
65	Electron Probe Microanalysis of REE in Eudialyte Group Minerals: Challenges and Solutions. Microscopy and Microanalysis, 2015, 21, 1096-1113.	0.4	5
66	Nature and distribution of PGE mineralisation in gabbroic rocks of the Lusatian Block, Saxony, Germany. Zeitschrift Der Deutschen Gesellschaft Fur Geowissenschaften, 2015, 166, 35-53.	0.4	7
67	Re–Os geochronology on sulfides from the Tudun Cu–Ni sulfide deposit, Eastern Tianshan, and its geological significance. International Journal of Earth Sciences, 2015, 104, 2241-2252.	1.8	12
68	Origin of Cu-Ni-PGE Mineralization at the Manchego Prospect, West Musgrave Province, Western Australia. Economic Geology, 2015, 110, 2063-2085.	3.8	9
69	Leaching of copper from Kupferschiefer by glutamic acid and heterotrophic bacteria. Minerals Engineering, 2015, 75, 38-44.	4.3	14
70	Distribution of Sb minerals in the Cu and Zn flotation of Rockliden massive sulphide ore in north-central Sweden. Minerals Engineering, 2015, 82, 125-135.	4.3	14
71	Paleoarchean sulfur cycling: Multiple sulfur isotope constraints from the Barberton Greenstone Belt, South Africa. Precambrian Research, 2015, 267, 311-322.	2.7	28
72	Formation of Mississippi Valley–type deposits linked to hydrocarbon generation in extensional tectonic settings: Evidence from the Jabali Zn-Pb-(Ag) deposit (Yemen). Geology, 2015, , G37112.1.	4.4	7

#	Article	IF	CITATIONS
73	A review of rare earth minerals flotation: Monazite and xenotime. International Journal of Mining Science and Technology, 2015, 25, 877-883.	10.3	72
74	Monazite geochronology and geothermobarometry in polymetamorphic host rocks of volcanic-hosted massive sulphide mineralizations in the Mesoproterozoic Areachap Terrane, South Africa. Journal of African Earth Sciences, 2015, 111, 258-272.	2.0	6
75	Bioleaching of Kupferschiefer blackshale – A review including perspectives of the Ecometals project. Minerals Engineering, 2015, 75, 116-125.	4.3	33
76	DEPOSITIONAL ENVIRONMENT AND LITHOSTRATIGRAPHY OF THE PALEOPROTEROZOIC MOOIDRAAI FORMATION, KALAHARI MANGANESE FIELD, SOUTH AFRICA. South African Journal of Geology, 2014, 117, 173-192.	1.2	12
77	Characterisation of graphite by automated mineral liberation analysis. Institutions of Mining and Metallurgy Transactions Section C: Mineral Processing and Extractive Metallurgy, 2014, 123, 184-189.	0.6	10
78	PGE geochemistry of the Fengshan porphyry–skarn Cu–Mo deposit, Hubei Province, Eastern China. Ore Geology Reviews, 2014, 56, 1-12.	2.7	14
79	On the geological availability of germanium. Mineralium Deposita, 2014, 49, 471-486.	4.1	87
80	PROVENANCE OF THE NEOPROTEROZOIC ROCKS OF THE GIFBERG GROUP (WESTERN SOUTH AFRICA). South African Journal of Geology, 2014, 117, 45-66.	1.2	3
81	Sulfur sources of sedimentary "buckshot―pyrite in the Auriferous Conglomerates of the Mesoarchean Witwatersrand and Ventersdorp Supergroups, Kaapvaal Craton, South Africa. Mineralium Deposita, 2014, 49, 751-775.	4.1	19
82	Evaluation of mineral processing by assessment of liberation and upgrading. Minerals Engineering, 2013, 53, 171-173.	4.3	28
83	The Composition and Depositional Environments of Mesoarchean Iron Formations of the West Rand Group of the Witwatersrand Supergroup, South Africa. Economic Geology, 2013, 108, 111-134.	3.8	85
84	Geological variations in the Merensky Reef at Bafokeng Rasimone Platinum Mine and its influence on flotation performance. Minerals Engineering, 2013, 52, 155-168.	4.3	7
85	Bimodal volcanism at the western margin of the Kaapvaal Craton in the aftermath of collisional events during the Namaqua-Natal Orogeny: The Koras Group, South Africa. Precambrian Research, 2012, 200-203, 163-183.	2.7	24
86	REE redistribution during hydrothermal alteration of ores of the Kalahari Manganese Deposit. Ore Geology Reviews, 2012, 47, 126-135.	2.7	23
87	Nature and origin of the protolith succession to the Paleoproterozoic Serra do Navio manganese deposit, Amapa Province, Brazil. Ore Geology Reviews, 2012, 47, 59-76.	2.7	22
88	Timing of supergene enrichment of low-grade sedimentary manganese ores in the Kalahari Manganese Field, South Africa. Ore Geology Reviews, 2012, 47, 136-153.	2.7	20
89	2.05-Ga Isotopic Ages for Transvaal Mississippi Valley–Type Deposits: Evidence for Large-Scale Hydrothermal Circulation around the Bushveld Igneous Complex, South Africa. Journal of Geology, 2011, 119, 69-80.	1.4	31
90	Sedimentary Provenance of the Neoarchean Ventersdorp Supergroup, Southern Africa: Shedding Light on the Evolution of the Kaapvaal Craton during the Neoarchean. Journal of Geology, 2011, 119, 575-596.	1.4	14

#	Article	IF	CITATIONS
91	Age and primary architecture of the Copperton Zn-Cu VMS deposit, Northern Cape Province, South Africa. Ore Geology Reviews, 2011, 39, 164-179.	2.7	12
92	PETROGRAPHY, GEOCHEMISTRY AND GEOCHRONOLOGY OF THE METAVOLCANIC ROCKS OF THE MESOPROTEROZOIC LEERKRANS FORMATION, WILGENHOUTSDRIF GROUP, SOUTH AFRICA - BACK-ARC BASIN TO THE AREACHAP VOLCANIC ARC. South African Journal of Geology, 2011, 114, 167-194.	1.2	13
93	Age of ferroan A-type post-tectonic granitoids of the southern part of the Keimoes Suite, Northern Cape Province, South Africa. Journal of African Earth Sciences, 2011, 60, 153-174.	2.0	24
94	From BIF to red beds: Sedimentology and sequence stratigraphy of the Paleoproterozoic Koegas Subgroup (South Africa). Sedimentary Geology, 2011, 236, 25-44.	2.1	53
95	PALEOENVIRONMENTAL CONTROLS ON THE TEXTURE AND CHEMICAL COMPOSITION OF PYRITE FROM NON-CONGLOMERATIC SEDIMENTARY ROCKS OF THE MESOARCHEAN WITWATERSRAND SUPERGROUP, SOUTH AFRICA. South African Journal of Geology, 2010, 113, 195-228.	1.2	62
96	Zoning of platinum group mineral assemblages in the UG2 chromitite determined through in situ SEM-EDS-based image analysis. Mineralium Deposita, 2010, 45, 147-159.	4.1	31
97	Sulfur isotope characteristics of metamorphosed Zn–Cu volcanogenic massive sulfides in the Areachap Group, Northern Cape Province, South Africa. Mineralium Deposita, 2010, 45, 481-496.	4.1	24
98	Lithogeochemistry as a tracer of the tectonic setting, lateral integrity and mineralization of a highly metamorphosed Mesoproterozoic volcanic arc sequence on the eastern margin of the Namaqua Province, South Africa. Lithos, 2010, 119, 345-362.	1.4	33
99	Correlation of Ordovician diamictites from Argentina and South Africa using detrital zircon dating. Journal of the Geological Society, 2010, 167, 217-220.	2.1	25
100	Deciphering formation processes of banded iron formations from the Transvaal and the Hamersley successions by combined Si and Fe isotope analysis using UV femtosecond laser ablation. Geochimica Et Cosmochimica Acta, 2010, 74, 2677-2696.	3.9	138
101	Evidence for an early Archaean granite from Bastar craton, India. Journal of the Geological Society, 2009, 166, 193-196.	2.1	117
102	Intrusive origin for Upper Group (UG1, UG2) stratiform chromitite seams in the Dwars River area, Bushveld Complex, South Africa. Mineralogy and Petrology, 2009, 97, 75-94.	1.1	108
103	Correlating multiple Neoarchean–Paleoproterozoic impact spherule layers between South Africa and Western Australia. Precambrian Research, 2009, 169, 100-111.	2.7	32
104	Reconstructing Earth's surface oxidation across the Archean-Proterozoic transition. Geology, 2009, 37, 399-402.	4.4	247
105	A NEW CHRONOSTRATIGRAPHIC PARADIGM FOR THE AGE AND TECTONIC HISTORY OF THE MESOPROTEROZOIC BUSHMANLAND ORE DISTRICT, SOUTH AFRICAA DISCUSSION. Economic Geology, 2009, 104, 1277-1281.	3.8	4
106	Genesis of High-Grade Iron Ores of the Archean Iron Ore Group around Noamundi, India. Economic Geology, 2008, 103, 365-386.	3.8	84
107	The Vergenoeg: Gauteng Province, South Africa Fluorite Mine. Rocks and Minerals, 2008, 83, 410-421.	0.1	3
108	Origin and Paleoenvironmental Significance of Major Iron Formations at the		48

Archean-Paleoproterozoic Boundary., 2008, , .

#	Article	IF	CITATIONS
109	Isotopic evidence for iron mobilization during Paleoproterozoic lateritization of the Hekpoort paleosol profile from Gaborone, Botswana. Earth and Planetary Science Letters, 2007, 256, 577-587.	4.4	47
110	Geochemistry of bedded barite of the Mesoproterozoic Aggeneys-Gamsberg Broken Hill-type district, South Africa. Mineralium Deposita, 2007, 42, 537-549.	4.1	19
111	Geochemical patterns of schists from the Bushmanland Group: An artificial neural networks approach. Journal of Geochemical Exploration, 2006, 91, 81-98.	3.2	9
112	Spatial and temporal distribution of microbially induced sedimentary structures: A case study from siliciclastic storm deposits of the 2.9Ga Witwatersrand Supergroup, South Africa. Precambrian Research, 2006, 146, 35-44.	2.7	69
113	The Paleoproterozoic carbonate-hosted Pering Zn–Pb deposit, South Africa: I. Styles of brecciation and mineralization. Mineralium Deposita, 2006, 40, 664-685.	4.1	14
114	The Paleoproterozoic carbonate-hosted Pering Zn–Pb deposit, South Africa. II: fluid inclusion, fluid chemistry and stable isotope constraints. Mineralium Deposita, 2006, 40, 686-706.	4.1	33
115	Carbonic fluid inclusions in Paleoproterozoic carbonate-hosted Zn-Pb deposits in Griqualand West, South Africa. South African Journal of Geology, 2006, 109, 55-62.	1.2	7
116	The chemostratigraphy of a Paleoproterozoic MnF- BIF succession -the Voelwater Subgroup of the Transvaal Supergroup in Griqualand West, South Africa. South African Journal of Geology, 2006, 109, 63-80.	1.2	32
117	Cretaceous Karstic Cave-Fill Manganese-Lead-Barium Deposits of Imini, Morocco. Economic Geology, 2006, 101, 385-405.	3.8	26
118	Links of organic carbon cycling and burial to depositional depth gradients and establishment of a snowball Earth at 2.3Ga. Evidence from the Timeball Hill Formation,Transvaal Supergroup, South Africa South African Journal of Geology, 2006, 109, 109-122.	1.2	31
119	Paleomagnetism of the lower two unconformity-bounded sequences of the Waterberg Group, South Africa: Towards a better-defined apparent polar wander path for the Paleoproterozoic Kaapvaal Craton South African Journal of Geology, 2006, 109, 157-182.	1.2	36
120	Precise SHRIMP U-Pb zircon age constraints on the lower Waterberg and Soutpansberg Groups, South African Journal of Geology, 2006, 109, 139-156.	1.2	55
121	Organotemplate structures in sedimentary manganese carbonates of the Neoproterozoic Penganga Group, Adilabad, India. Journal of Earth System Science, 2005, 114, 247-257.	1.3	6
122	Archean seismites of the Ventersdorp Supergroup, South Africa. South African Journal of Geology, 2005, 108, 345-350.	1.2	10
123	New interpretation of the origin of tiger's-eye: Comment and Reply. Geology, 2004, 32, e44-e45.	4.4	0
124	Organotemplate silica deposition in Neoproterozoic deep-marine environments: evidence from the Penganga Group, Adilabad, India. Terra Nova, 2004, 16, 338-343.	2.1	8
125	Mineral chemistry of sphalerite and galena from Pb-Zn mineralization hosted by the Transvaal Supergroup in Griqualand West, South Africa. South African Journal of Geology, 2004, 107, 341-354.	1.2	10
126	Ancient sub-seafloor alteration of basaltic andesites of the Ongeluk Formation, South Africa: implications for the chemistry of Paleoproterozoic seawater. Chemical Geology, 2003, 201, 37-53.	3.3	43

#	Article	IF	CITATIONS
127	Tropical laterites, life on land, and the history of atmospheric oxygen in the Paleoproterozoic. Geology, 2002, 30, 491.	4.4	143
128	Red Bed-Hosted Oncolitic Manganese Ore of the Paleoproterozoic Soutpansberg Group, Bronkhorstfontein, South Africa. Economic Geology, 2002, 97, 1151-1166.	3.8	14
129	Manganvesuvianite and tweddillite, two new Mn3+-silicate minerals from the Kalahari manganese fields, South Africa. Mineralogical Magazine, 2002, 66, 137-150.	1.4	42
130	Spectacular Minerals from the Kalahari Manganese Field, South Africa. Rocks and Minerals, 2002, 77, 94-107.	0.1	1
131	Acceptance of the Waldemar Lindgren Award for 2002. Economic Geology, 2002, 97, 1624-1625.	3.8	0
132	Formation of jasper and andradite during low-temperature hydrothermal seafloor metamorphism, Ongeluk Formation, South Africa. Contributions To Mineralogy and Petrology, 2001, 142, 27-42.	3.1	35
133	Late Paleoproterozoic Mn-rich oncoids: Earliest evidence for microbially mediated Mn precipitation. Geology, 2001, 29, 835.	4.4	19
134	Structure, compressibility, hydrogen bonding, and dehydration of the tetragonal Mn ³⁺ hydrogarnet, henritermierite. American Mineralogist, 2001, 86, 147-158.	1.9	34
135	THE MANGANESE FORMATION OF THE NEOPROTEROZOIC PENGANGA GROUP, INDIA—REVISION OF AN ENIGMA—A REPLY. Economic Geology, 2000, 95, 239-240.	3.8	7
136	Paleoproterozoic snowball Earth: Extreme climatic and geochemical global change and its biological consequences. Proceedings of the National Academy of Sciences of the United States of America, 2000, 97, 1400-1405.	7.1	379
137	Supergene Ferromanganese Wad Deposits Derived from Permian Karoo Strata along the Late Cretaceous-Mid-Tertiary African Land Surface, Ryedale, South Africa. Economic Geology, 2000, 95, 203-220.	3.8	34
138	Fluid inclusion studies in cogenetic hematite, hausmannite, and gangue minerals from high-grade manganese ores in the Kalahari manganese field, South Africa. Economic Geology, 1999, 94, 589-595.	3.8	30
139	Earliest laterites and possible evidence for terrestrial vegetation in the Early Proterozoic. Geology, 1998, 26, 263.	4.4	64
140	The manganese formation of the Neoproterozoic Penganga Group, India; revision of an enigma. Economic Geology, 1998, 93, 1091-1102.	3.8	41
141	Mineral paragenesis of the Kalahari managanese field, South Africa. Ore Geology Reviews, 1996, 11, 405-428.	2.7	88
142	Karst-hosted fresh-water Paleoproterozoic manganese deposits, Postmasburg, South Africa. Economic Geology, 1996, 91, 1435-1454.	3.8	22
143	Influence of Carbonate Solubilisation on Copper Leaching from Kupferschiefer with Organic Acids. Advanced Materials Research, 0, 1130, 278-281.	0.3	0
144	Bundling Analytical Capacities to Understand Phase Formation in Recycling of Functional Materials. Materials Science Forum, 0, 959, 183-190.	0.3	1

#	Article	IF	CITATIONS
145	Cues to Greater Recycling Efficiency - Characterization of a Crushed Mobile Phone by Mineral Liberation Analysis (MLA). Materials Science Forum, 0, 959, 134-141.	0.3	4